DENOISING BASED ON NON LOCAL MEANS FOR ULTRASOUND IMAGES WITH SIMULTANEOUS MULTIPLE NOISE DISTRIBUTIONS

Denis H. P. Salvadeo[†⋆], Isabelle Bloch[‡], Florence Tupin[‡], Nelson D. A. Mascarenhas[⋆],
Alexandre L. M. Levada[⋆], Charles-Alban Deledalle[∗], Sonia Dahdouh [‡]

[†] São Paulo State University, DEMAC, Rio Claro, Brazil
[⋆] Federal University of São Carlos, Computer Department, São Carlos, Brazil
[‡] Institut Mines-Télécom, Télécom ParisTech, CNRS LTCI, Paris, France
[∗] Université Bordeaux 1, Institut de Mathématiques de Bordeaux, Talence, France

ABSTRACT

In this paper, an extension of the framework proposed by Deledalle *et al.*[1] for Non Local Means (NLM) method is proposed. This extension is a general adaptive method to denoise images containing multiple noises. It takes into account a segmentation stage that indicates the noise type of a given pixel in order to select the similarity measure and suitable parameters to perform the denoising task, considering a certain patch on the image. For instance, it has been experimentally observed that fetal 3D ultrasound images are corrupted by different types of noise, depending on the tissue. Finally, the proposed method is applied to denoise these images, showing very good results.

Index Terms— ultrasound image, image denoising, non local means, multiple noises, ultrasound segmentation

1. INTRODUCTION

Ultrasound images are known to be very noisy, and the usual assumption is that pixel intensities follow a Rayleigh distribution [2, 3, 4]. However, it was identified by Anquez [5] that in fetal 3D ultrasound (US) images, different noise distributions characterize different tissues appearances, depending on pixel intensity saturation and tissue type. For example, it is shown that the noise is governed by a Gaussian distribution in fetus tissues and by an Exponential distribution in amniotic fluid area (in the saturated case).

This analysis can be extended by using the Chi-Square test to verify the fitting of the histogram data of each tissue or class to some distributions and the Method of Moments for parameter estimation of these distributions. In our examples, the US image can be separated in two classes only, namely Dark (DA) and Light (LA) (see Fig. 1).

The LA class, comprising fetus and light regions of other tissues of a pregnant woman (OP) such as placenta and outside it, is corrupted by Gaussian noise (independent of the saturation level), whereas DA class, comprising amniotic fluid and dark areas of OP, is corrupted by Rayleigh, Gamma or Exponential distributed noise, depending on whether the image is saturated or not. So, the Chi-Square test could be used to determine the best fit among these distributions for DA.

Therefore, an adaptive method to denoise these images taking into account the different distributions is necessary. In order to pro-
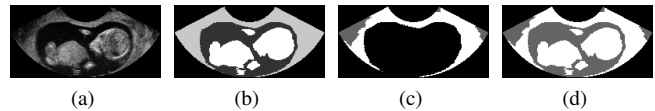
Fig. 1. Segmented Image for analysis: (a) Original image, (b) Manually segmented images in three classes (fetus, amniotic fluid and other tissues of pregnant woman), (c) Dark and light areas from other tissues of pregnant woman and (d) Manually segmented images in two classes (Light and Dark areas).

pose such a method, a state-of-art Non Local Means (NLM) approach is adapted in this work, extending the framework proposed by Deledalle *et al.* [1], to refine the NLM weights according to the noise distribution.

This paper describes the proposed 2D method and discusses some denoising results on fetal ultrasound images to evaluate it. However, despite its application for US images, the proposed method is general. Indeed, it is important to highlight that it could be useful in other domains where different classes of noise distributions have to be taken into account or where a higher number of classes has to be considered.

Note that the aim of denoising in this paper is not to improve the visual inspection by medical experts (who are used to interpret the images with speckle noise), but to facilitate the automated segmentation.

Finally, this text is organized as follows. Section 2 presents the considered Non Local Means approach. Section 3 describes the proposed adaptive method to denoise ultrasound images. Finally, some experiments and results on fetal ultrasound images are described in Section 4 and a final discussion is presented in Section 5.

2. NON LOCAL MEANS

The classical NLM method was proposed in [6] and is mainly based on the redundancy of patches in images. In this method, the noise-free value of a pixel is basically estimated as a weighted mean of pixels in a certain region. These weights are calculated using a Euclidean distance to measure the similarity between a central patch and neighboring patches in a search window, where the central pixel of both the central patch and the search window is the current pixel to be estimated. As the classical method is based on the Euclidean distance, it is suitable for Additive White Gaussian Noise (AWGN).

This method can be represented by the following equation [6]:

$$\hat{u}_s \triangleq \frac{\sum_{t \in W} \omega(s,t) v_t}{\sum_{t \in W} \omega(s,t)}, \quad (1)$$

where $\hat{u}_s$ is a current noise-free estimation of the value of the pixel at position s, v_t is a noisy value of a pixel t belonging to a search window W and $\omega(s,t)$ are the weights comparing the patches centered at s and t and defined by [6, 7]:

$$\omega(s,t) \triangleq \exp\left(-\frac{1}{h}\sum_k |v_{s,k} - v_{t,k}|^2\right), \quad (2)$$

where h controls the exponential decay, $v_{s,k}$ and $v_{t,k}$ are the k-th pixel in the patches s and t from noisy image v, respectively.

In order to apply this simple idea to other noise models and to improve the results, a framework was proposed in [1] to iteratively generate and refine the weights based on Weighted Maximum Likelihood estimation. This method is derived from the following equation in a Bayesian Framework

$$\omega(s,t)^{(i)} \triangleq \frac{p(\mathcal{H}_0|\boldsymbol{v_s},\boldsymbol{v_t},\hat{\boldsymbol{u}}^{(i-1)})}{p(\mathcal{H}_1|\boldsymbol{v_s},\boldsymbol{v_t},\hat{\boldsymbol{u}}^{(i-1)})} = \underbrace{\frac{p(\boldsymbol{v_s},\boldsymbol{v_t}|\mathcal{H}_0)}{p(\boldsymbol{v_s},\boldsymbol{v_t}|\mathcal{H}_1)}}_{\text{likelihood}} \times \underbrace{\frac{p(\mathcal{H}_0|\hat{\boldsymbol{u}}^{(i-1)})}{p(\mathcal{H}_1|\hat{\boldsymbol{u}}^{(i-1)})}}_{\text{a priori}}, \quad (3)$$

where $\mathcal{H}_0 : \boldsymbol{u}_1 = \boldsymbol{u}_2 \equiv \boldsymbol{u}_{12}$ is the null hypothesis, $\mathcal{H}_1 : \boldsymbol{u}_1 \neq \boldsymbol{u}_2$ is the alternative hypothesis, $\boldsymbol{v_s}$ and $\boldsymbol{v_t}$ are noisy patches, $\boldsymbol{u}_1$ and $\boldsymbol{u}_2$ are the noise-free patches, $\boldsymbol{u}_{12}$ is a common parameter and $\hat{\boldsymbol{u}}^{(i-1)}$ is a noise-free image estimated in the previous iteration.

Assuming that the pixels inside a patch are independent of each other conditionally to the class, two similarity measures were directly derived: the Generalized Likelihood Ratio (GLR) and Symmetric Kullback-Leibler Divergence (SKLD), respectively.

The GLR is defined in [8]:

$$\mathcal{L}_G(\boldsymbol{v_1}, \boldsymbol{v_2}) = \frac{\sup_{\boldsymbol{t}} p(\boldsymbol{v_1}, \boldsymbol{v_2}|\boldsymbol{u}_{12} = \boldsymbol{t}, \mathcal{H}_0)}{\sup_{\boldsymbol{t_1},\boldsymbol{t_2}} p(\boldsymbol{v_1}, \boldsymbol{v_2}|\boldsymbol{u}_1 = \boldsymbol{t_1}, \boldsymbol{u}_2 = \boldsymbol{t_2}, \mathcal{H}_1)}. \quad (4)$$

In turn, the SKLD is defined in [1]:

$$\mathcal{D}_{KL}(\boldsymbol{u_1}, \boldsymbol{u_2}) = \int (p(\boldsymbol{v}|\boldsymbol{u_1}) - p(\boldsymbol{v}|\boldsymbol{u_2})) \log \frac{p(\boldsymbol{v}|\boldsymbol{u_1})}{p(\boldsymbol{v}|\boldsymbol{u_2})} d\boldsymbol{v}. \quad (5)$$

Assuming uncorrelated noise, the similarity between patches corresponds then to a product of the similarities between their pixels. Thus, taking the log of this product, the joint similarity measure can be defined by [1]:

$$\omega(s,t)^{(i)} = \phi\left[-\sum_k \left(\frac{-\log \mathcal{L}_G(v_{s,k}, v_{t,k})}{\alpha} - \frac{\mathcal{D}_{KL}(\hat{u}_{s,k}^{(i-1)}, \hat{u}_{t,k}^{(i-1)})}{\beta}\right)\right]. \quad (6)$$

where ϕ is a kernel (usually defined as an exponential or a trapezoidal kernel) and α and β are confidence parameters in the amount of filtering and pre-estimated image, respectively. It is worth noting that the pre-estimated image in the first iteration can be defined as non iterative NLM. This initial condition corresponds to define the pre-estimated images as a matrix of constant values equal to 1 and the first value of β equal to 1. Besides if the noise is Gaussian, it corresponds to the classical NLM of Buades *et al.* [6].

Table 1 summarizes the GLR and SKLD of Gaussian, Rayleigh and Gamma distributions. Also, these measures for Gamma distribution are the same for Exponential distribution, since the latter is a special case of the former. In addition, Fig. 2 summarizes the weights from individual and joint similarity measures. The graphs

Table 1. GLR and SKLD for some distributions.

Distribution	GLR	SKLD	NLM
Gaussian	$e^{-(v_1-v_2)^2}$	$-(\hat{u}_1 - \hat{u}_2)^2$	$\frac{\sum_{t \in W} \omega(s,t) v_t}{\sum_{t \in W} \omega(s,t)}$
Rayleigh	$\frac{v_1 v_2}{v_1^2 + v_2^2}$	$\frac{\hat{u}_1^2}{\hat{u}_2^2} + \frac{\hat{u}_2^2}{\hat{u}_1^2} - 2$	$\sqrt{\frac{\sum_{t \in W} \omega(s,t) v_t^2}{\sum_{t \in W} \omega(s,t)}}$
Gamma	$\frac{v_1 v_2}{(v_1 + v_2)^2}$	$\frac{(\hat{u}_1 - \hat{u}_2)^2}{\hat{u}_1 \hat{u}_2}$	$\frac{\sum_{t \in W} \omega(s,t) v_t}{\sum_{t \in W} \omega(s,t)}$

in this figure represent the obtained values of the similarity measures described in Table 1 (as well as the weights generated by a exponential kernel), when the difference between the intensities of the two pixels increases. It is important to note that in these graphs $-\log \mathcal{L}_G(v_{s,k}, v_{t,k})$ is used rather than GLR only, for reasons of simplicity. More details on GLR and SKLD can be found in [1, 8].
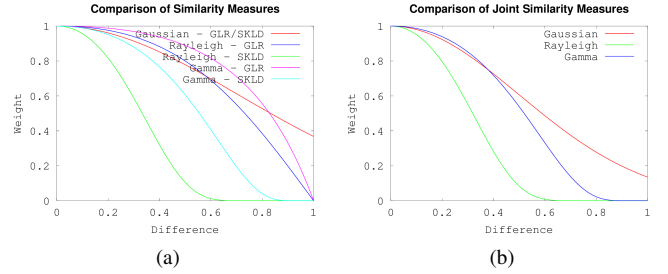
Fig. 2. Comparison of (a) Similarity Measures and (b) Joint Similarity Measures in terms of weights.

Finally, an extension to adapt this method for a multi-distribution image is proposed in the next section.

3. THE PROPOSED ADAPTIVE METHOD

In this section, an extension of the framework proposed in [1] for images containing multi-distribution noise is presented. To apply the most suitable similarity measure for SKLD and GLR for each pixel, its distribution noise should be determined previously. So, assuming that we have a pixel classification such that pixels corrupted by the same noise distribution are in the same class, we can rewrite the framework equations to consider this information. Thus, let $\boldsymbol{L}$ be a classification of an image according to the noise distribution at each pixel, then Eqs. 3 and 6 can be rewritten as, respectively:

$$\omega(s,t)^{(i)} \triangleq \frac{p_L(\mathcal{H}_0|\boldsymbol{v_s},\boldsymbol{v_t},\hat{\boldsymbol{u}}^{(i-1)})}{p_L(\mathcal{H}_1|\boldsymbol{v_s},\boldsymbol{v_t},\hat{\boldsymbol{u}}^{(i-1)})} = \underbrace{\frac{p_L(\boldsymbol{v_s},\boldsymbol{v_t}|\mathcal{H}_0)}{p_L(\boldsymbol{v_s},\boldsymbol{v_t}|\mathcal{H}_1)}}_{\text{likelihood}} \times \underbrace{\frac{p_L(\mathcal{H}_0|\hat{\boldsymbol{u}}^{(i-1)})}{p_L(\mathcal{H}_1|\hat{\boldsymbol{u}}^{(i-1)})}}_{\text{a priori}}, \quad (7)$$

$$\omega(s,t)^{(i)} = \phi_{L_s}\left[-\sum_k \left(\frac{-\log \mathcal{L}_G^{(L_{s,k})}(v_{s,k}, v_{t,k})}{\alpha_{L_{s,k}}} - \frac{\mathcal{D}_{KL}^{(L_{s,k})}(\hat{u}_{s,k}^{(i-1)}, \hat{u}_{t,k}^{(i-1)})}{\beta_{L_{s,k}}}\right)\right], \quad (8)$$

where ϕ_{L_s} is a kernel for noise distribution L on s-th pixel, $\mathcal{L}_G^{(L_{s,k})}$ and $\mathcal{D}_{KL}^{(L_{s,k})}$ are the GLR and SKLD (similarity measures) for the noise distribution L on k-th pixel from the patch defined by s, respectively, and $\alpha_{L_{s,k}}$ and $\beta_{L_{s,k}}$ are confidence parameters in the filtering quantity and pre-estimated image for the noise distribution L on k-th pixel from the patch defined by s, respectively. It is worth to note that if an image is represented by a single noise distribution, we obtain the original equations defined in [1]. So, the extended algorithm, namely 2D-DirectAdapt, is presented in Algorithm 1.

Here, all patches within a given search window are considered, even if they belong to different classes or cover several classes. Also,

Input: - noisy image $\boldsymbol{v}$
    - pre-estimated image $\boldsymbol{u'}$
    - 2D-FFT (Fast Fourier Transform) of the patch shape $\mathcal{F}(\boldsymbol{S})$
    - seach window $\boldsymbol{W}$
    - contributions of similarity on noisy image $\alpha_{L_{s,k}}$
    - contributions of similarity on pre-estimated image $\beta_{L_{s,k}}$
    - segmented image according to noise type classes $\boldsymbol{L}$
Output: - estimated noise-free image $\hat{\boldsymbol{u}}$

1 Initialize the accumulator images $\boldsymbol{A}$ and $\boldsymbol{B}$ to zero
2 **forall the** *shift δ in the W* **do**

3   Compute $\Delta_{\boldsymbol{v},\delta}(s) = \dfrac{-\log \mathcal{L}_G^{(L_s)}(\boldsymbol{v}(s), \boldsymbol{v}(s+\delta))}{\alpha_{L_s+\delta}}$ for all pixels s in $\boldsymbol{v}$

4   Compute $\Delta_{\boldsymbol{u'},\delta}(s) = \dfrac{\mathcal{D}_{KL}^{(L_s)}(\boldsymbol{u'}(s), \boldsymbol{u'}(s+\delta))}{\beta_{L_s+\delta}}$ for all pixels s in $\boldsymbol{u'}$

5   Compute the 2-D FFT $\mathcal{F}\left(\Delta_{\boldsymbol{v},\delta}(s)\right)$ and $\mathcal{F}\left(\Delta_{\boldsymbol{u'},\delta}(s)\right)$

6   Perform the convolution of $\Delta_{\boldsymbol{v},\delta}(s)$ and $\Delta_{\boldsymbol{u'},\delta}(s)$ by the shape $\boldsymbol{S}$:

        $d_{\boldsymbol{v}}(.,.+\delta) = \mathcal{F}^{-1}\left(\overline{\mathcal{F}(\boldsymbol{S})}\mathcal{F}\left(\Delta_{\boldsymbol{v},\delta}(s)\right)\right)(.)$

        $d_{\boldsymbol{u'}}(.,.+\delta) = \mathcal{F}^{-1}\left(\overline{\mathcal{F}(\boldsymbol{S})}\mathcal{F}\left(\Delta_{\boldsymbol{u'},\delta}(s)\right)\right)(.)$

7   **forall the** *pixels s* **do**
8   Compute the weights:

        $\omega(s, s+\delta) = \phi_{L_s}\left(-\left(d_{\boldsymbol{v}}(s, s+\delta) + d_{\boldsymbol{u'}}(s, s+\delta)\right)\right)$

9   Update the accumulators:
        $\boldsymbol{A}(s) = \boldsymbol{A}(s) + \omega(s, s+\delta)\boldsymbol{v}(s)$ according NLM for L_s in Table 1
        $\boldsymbol{A}(s) = \boldsymbol{A}(s) + \omega(s, s+\delta)$
    end
  end

10 $\hat{\boldsymbol{u}}(s) = \dfrac{\boldsymbol{A}(s)}{\boldsymbol{B}(s)}$ for all pixels s, according NLM for L_s in Table 1

Algorithm 1: 2D-DirectAdapt. Based on [7].

Fig. 3. Block diagram of the proposed methodology to denoise fetal ultrasound images.

Table 2. Denoising results for synthetic images.

Methods	PSNR	SSIM
Noisy	11.92	0.10
BM3D ($\sigma^2 = 0.36$)	20.62	**0.74**
BM3D ($\sigma^2 = 0.40$)	20.63	**0.74**
NLM for Gamma ($\alpha = 0.29, \beta = 0.29$)	21.98	0.66
NLM for Gamma ($\alpha = 0.18, \beta = 0.18$)	22.55	0.62
NLM for Rayleigh ($\alpha = 0.30, \beta = 0.30$)	18.98	0.66
NLM for Rayleigh ($\alpha = 0.14, \beta = 0.14$)	18.52	0.45
NLM for Gaussian ($\alpha = 0.41, \beta = 0.41$)	21.24	0.62
2D-DirectAdapt (RAY $= 0.27$, GAM $= 0.26$, GAU $= 0.10$, EXP $= 0.45$)	24.41	0.67
2D-DirectAdapt (RAY $= 0.15$, GAM $= 0.15$, GAU $= 0.07$, EXP $= 0.26$)	**25.06**	0.57

note that the similarity between two noisy patches $\boldsymbol{v}_s$ and $\boldsymbol{v}_t$ is defined as the sum of the similarities between $v_{s,k}$ and $v_{t,k}$ according to the type of noise on $v_{s,k}$ (similarly for SKLD). This enables to consider multi-class patches.
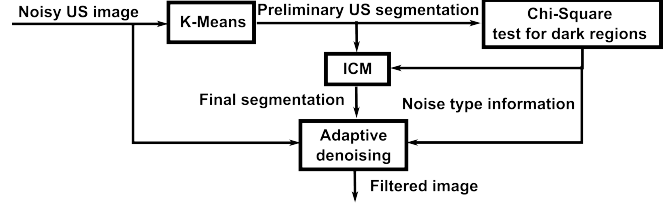
In turn, to obtain the optimal thresholding of a fetal ultrasound image, it is important to define the distribution D of pixels in Dark Area (amniotic fluid and dark regions of the mother's body) along the image. Basically, this region can be corrupted by Exponential, Rayleigh or Gamma Distribution. To determine which among these distributions fits better the Dark Area, a Chi-Square test can be used.

Based on the work by Anquez in [5], where it is shown that the K-means produce satisfying segmentation results for our images, we have also tested it to obtain an initial segmentation. Basically, the class with the centroid corresponding to the lowest mean shows high correspondence with the amniotic fluid and darker tissues of the mother. In turn, the class with the centroid corresponding to the highest mean shows high correspondence to the fetus and lighter parts of the mother. So, the Chi-Square test can be applied on DA.

Once this is done, spatial regularization is achieved using a Markov Random Field model (using a Potts model), solved using the Iterated Conditional Modes (ICM) algorithm [9] for maximum *a posteriori* (MAP) estimation. The estimation of the Beta parameter (spatial dependency parameter that controls the tradeoff between likelihood and prior knowledge) is done numerically as in the work of Levada [10, 11]. Therefore, this optimal segmentation contains two classes, Dark Area and Light Area, that are described by D and Gaussian distribution (likelihoods for each class used in ICM), respectively. ICM is a deterministic method, which usually converges in a few iterations. However, its result is dependent on the initial estimate of the classes. Note that a more efficient method to do this optimization step such as graph-cuts [12] can be used.

It is noteworthy that only an initial rough classification is required here, which justifies the choice of unsupervised and simple methods for this task. In addition, the focus of this work is to evaluate the adaptive denoising method only.

So, the proposed methodology can be summarized by the diagram in Fig. 3. Finally, based on what has been discussed so far, in the next section we discuss some results of the proposed method.

4. EXPERIMENTS AND RESULTS

In this section, some results to evaluate the proposed method are presented and discussed. In all experiments a trapezoidal kernel was used.

In the first experiment, we consider a synthetic image, where different types of noise were applied depending of the segmentation pattern. Each class in this pattern corresponds to a different noise, totalizing four classes and four noise distributions: Rayleigh, Gaussian, Gamma and Exponential. To generate the noisy image here, a segmentation was considered, where for each region from the original image corresponding to each class, one kind of noise was applied. These noisy images were denoised by NLM for Gaussian Noise, 2D-DirectAdapt method and Block Matching and 3D Filtering (BM3D) [13]. For a quantitative evaluation, we computed the Peak Signal-to-Noise Ratio (PSNR) and the Structure Similarity Index (SSIM) measures [14].

The best denoising results and quantitative results in terms of SSIM and PSNR for each method in this experiment are shown in Fig. 4 and in Table 2. The settings used here were $W = 10 \times 10$, $P = 3 \times 3$ and 3 iterations for 2D-DirectAdapt and one iteration for NLM filters. Note that the proposed method was quantitatively and qualitatively superior to the basic NLM methods, showing very good results. Also, it is the best in terms of PSNR. But, despite the fact that BM3D was developed for AWGN, it also presents very good results in these images containing multiple noises, obtaining the best results in terms of SSIM. Also, observe that the 2D-DirectAdapt method preserved best the DC level of the image.

In the next experiment, real images from fetal ultrasound system are filtered using the proposed method. Its obtained results are compared to basic versions of NLM. The settings used here were $W = 10 \times 10$, $P = 3 \times 3$ and pairs ($\alpha = 0.02, \beta = 0.02$), ($\alpha = 0.05, \beta = 0.05$), ($\alpha = 0.05, \beta = 0.25$) for Gaussian, Gamma and Rayleigh distributions in all tested methods, whose results are shown in Fig. 5.

Finally, since there is no ground truth for quantitative comparison, the evaluation takes place in a visual way. Thus, it may be noticed that the results using the adaptive method (according to the actual distribution of the each tissue) provides a good balance be-
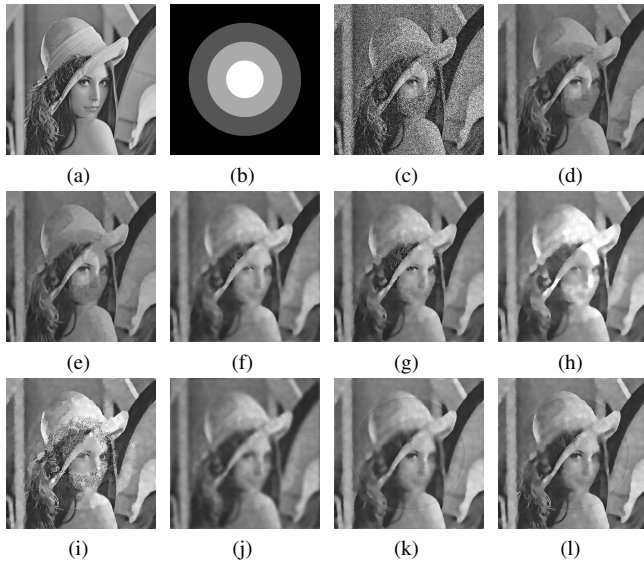
Fig. 4. Denoising results for synthetic image (c) generated according to segmentation in (b), where the regions of original image (a) corresponding to black, dark gray, light gray and white classes are corrupted by Rayleigh, Gamma, Exponential and Gaussian noise, respectively. The remaining items are filtered by (d)-(e) BM3D, (f)-(g) NLM for Gamma, (h)-(i) NLM for Rayleigh, (j) NLM for Gaussian and (k)-(l) 2D-DirectAdapt. The parameters are specified in Table 2.

tween details preservation and noise removal. This indicates that the use of an adaptive method based on NLM is promising for these types of images.

5. FINAL CONSIDERATIONS

In this paper, a simple adaptive extension of the NLM framework of [1], taking into account several noise distributions in the same image was proposed. For this purpose, a segmented image was considered such that each class corresponds to one type of noise distribution.

To evaluate the proposed method, it was applied on fetal ultrasound images, in which different tissues are corrupted by different noise distributions. The proposed method has obtained very good results.

Despite of the application of the proposed method in US images, it is important to reinforce that this is a general method.

As the main drawback of the proposed method we can highlight that the determination of the different parameters is done manually.

Finally, future works will include: 1) the automatic determination of the parameters, 2) the data decorrelation and subsequent learning of dedicated parameters similarly to what was done for Synthetic Aperture Radar (SAR) in [15], or modeling the local spatial dependence of data using second order statistics in a MRF model, and 3) an extensive quantitative evaluation of the adaptive method, in particular by checking the influence of filtering on subsequent segmentation steps.

6. REFERENCES

[1] C. Deledalle, L. Denis, and F. Tupin, "Iterative Weighted Maximum Likelihood Denoising With Probabilistic Patch-Based
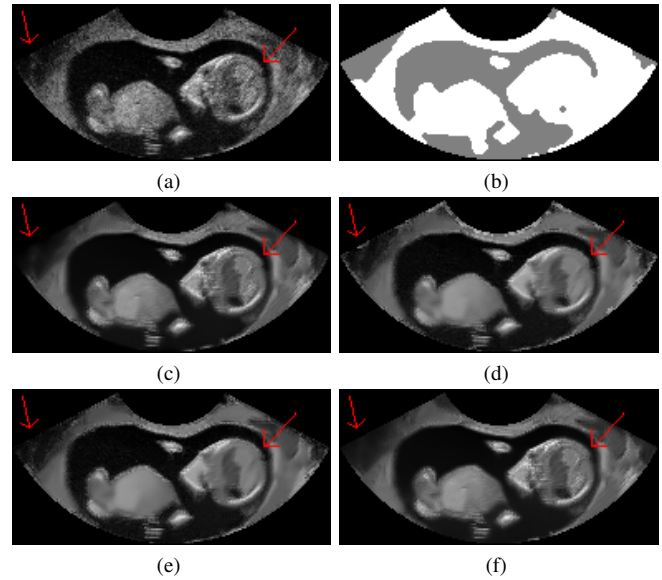
Fig. 5. Denoising results for real images: (a) noisy image, (b) Segmented Image by ICM, (c) NLM for Gaussian, (d) NLM for Rayleigh, (e) NLM for Gamma and (f) 2D-DirectAdapt.

Weights," *IEEE Transactions on Image Processing*, vol. 18, no. 12, pp. 2661–2672, 2009.

[2] R. F. Wagner, S. W. Smith, J. M. Sandrik, and H. Lopez, "Statistics of Speckle in Ultrasound B-Scans," *IEEE Transactions on Sonics and Ultrasonics*, vol. 30, no. 3, pp. 156–163, 1983.

[3] J. A. Noble and D. Boukerroui, "Ultrasound Image Segmentation: a Survey," *IEEE Transactions on Medical Imaging*, vol. 25, no. 8, pp. 987–1010, 2006.

[4] J. C. Seabra and J. M. Sanches, "On Estimating De-speckled and Speckle Components from B-mode Ultrasound Images," in *2010 IEEE International Symposium on Biomedical Imaging: From Nano to Macro*, 2010, pp. 284–287.

[5] J. Anquez, E. D. Angelini, G. Grange, and I. Bloch, "Automatic Segmentation of Antenatal 3-D Ultrasound Images," *IEEE Transactions on Biomedical Engineering*, vol. 60, no. 5, pp. 1388–1400, 2013.

[6] A. Buades, B. Coll, and J. M. Morel, "A Review of Image Denoising Algorithms, with a New One," *SIAM Multiscale Modeling & Simulation*, vol. 4, no. 2, pp. 490–530, 2005.

[7] C. Deledalle, V. Duval, and J. Salmon, "Non-local Methods with Shape-Adaptive Patches (NLM-SAP)," *Journal of Mathematical Imaging and Vision*, vol. 43, no. 2, pp. 103–120, 2012.

[8] C. Deledalle, L. Denis, and F. Tupin, "How to Compare Noisy Patches? Patch Similarity Beyond Gaussian Noise," *International Journal of Computer Vision*, vol. 99, no. 1, pp. 86–102, 2012.

[9] J. Besag, "On the Statistical Analysis of Dirty Pictures," *Journal of the Royal Statistical Society. Series B (Methodological)*, vol. 48, no. 3, pp. pp. 259–302, 1986.

[10] A. L. M. Levada, N. D. A. Mascarenhas, and A. Tannús, "A Novel MAP-MRF Approach for Multispectral Image Contextual Classification using Combination of Suboptimal Iterative

Algorithms," *Pattern Recognition Letters*, vol. 31, no. 13, pp. 1795 – 1808, 2010.

[11] A. L. M. Levada, N. D. A. Mascarenhas, and A. Tannús, "Pseudolikelihood Equations for Potts MRF Model Parameter Estimation on Higher Order Neighborhood Systems," *IEEE Geoscience and Remote Sensing Letters*, vol. 5, no. 3, pp. 522–526, 2008.

[12] Y. Boykov, O. Veksler, and R. Zabih, "Fast Approximate Energy Minimization via Graph Cuts," *IEEE Transactions on Pattern Analysis and Machine Intelligence*, vol. 23, no. 11, pp. 1222–1239, 2001.

[13] K. Dabov, A. Foi, V. Katkovnik, and K. Egiazarian, "Image Denoising by Sparse 3-D Transform-Domain Collaborative Filtering," *IEEE Transactions on Image Processing*, vol. 16, no. 8, pp. 2080–2095, 2007.

[14] Z. Wang and A. C. Bovik, "Mean Squared Error: Love it or Leave it? A New Look at Signal Fidelity Measures," *IEEE Signal Processing Magazine*, vol. 26, no. 1, pp. 98–117, 2009.

[15] C. Deledalle, L. Denis, F. Tupin, A. Reigber, and M. Jäger, "NL-SAR: a Unified Non-Local Framework for Resolution-Preserving (Pol)(In)SAR Denoising," *IEEE Transactions on Geoscience and Remote Sensing*, 2014, (to appear).